

Supporting Information for

Synthesis and Characterization of a Family of M^{2+} Complexes Supported
by a Trianionic ONO^{3-} Pincer Ligand: Towards the Stabilization of High-
Spin Square-Planar Complexes

*M. E. Pascualini,^a S. A. Stoian,^b A. Ozarowski,^b N. V. Di Russo,^a A. E.
Thuijs,^a K. A. Abboud,^a G. Christou^a and A. S. Veige^a*

^aDepartment of Chemistry, Center for Catalysis, University of Florida, Gainesville, FL
32611 (USA).

^bNational High Magnetic Field Laboratory, Florida State University, Tallahassee, FL
32310 (USA).

Table of Contents

1. General Considerations.....	3
2. Synthesis of 3.....	5
3. X-ray crystallography of 3.....	7
4. Synthesis of 4.....	10
5. X-ray crystallography of 4.....	12
6. Synthesis of 5.....	15
7. X-ray crystallography of 5.....	18
8. Magnetism Studies of 3 and 4.....	21
9. DFT Calculations of 4.....	23
10. Effective g-values predicted for 4 using equation 1.....	30
11. Cartesian Coordinates of the Geometry Optimized Structures.....	30
12. References.....	40

1. General Considerations.

Unless specified otherwise, all manipulations were performed under an inert atmosphere using standard Schlenk or glovebox techniques. Glassware was oven dried before use. Pentane, tetrahydrofuran (THF), Diethyl ether (Et₂O), and 1,2-dimethoxyethane (DME) were dried using a GlassContours drying column. Benzene-*d*₆ (Cambridge Isotopes) was dried over sodium-benzophenone ketyl and distilled or vacuum transferred and stored over 4 Å molecular sieves. MnCl₂ 99% (anhydrous) was purchased from Sigma-Aldrich, CoCl₂ 99% (anhydrous) and NiCl₂·DME 97% were purchased from Strem Chemicals, and used as received.

CV was performed under a nitrogen atmosphere using a standard three-electrode setup. A Pt mesh was used as a working electrode, a Pt wire was used as counter electrode, and Ag/AgCl was used as reference electrode. The measurements were made in 0.1 M Bu₄NPF₆ acetonitrile solution, and a 10 mM ferrocene solution was used as external reference. Bu₄NPF₆ 99.0% was purchased from Sigma-Aldrich and was used as received. Electrodes were purchased from either BASi, Inc. or CH Instruments, Inc. Potential sweeps were controlled by a Princeton Applied Research Versastat II potentiostat.

NMR spectra were obtained on Varian Mercury Broad Band 300 MHz, or Varian Mercury 300 MHz spectrometers. Chemical shifts are reported in δ (ppm). For ¹H and ¹³C{¹H} NMR spectra the solvent resonance was referenced as an internal reference. Elemental analyses were performed at Complete Analysis Laboratory Inc., Parsippany, New Jersey.

High-frequency EPR spectra were recorded using a home-built spectrometer at the EMR facility of NHMFL. The instrument is a transmission-type device in which waves

are propagated in cylindrical lightpipes. The microwaves were generated by a phase-locked oscillator (Virginia Diodes) operating at a frequency of 13 ± 1 GHz and generating its harmonics, of which the 4th, 8th, 16th, 24th and 32nd were available. A superconducting magnet (Oxford Instruments) capable of reaching a field of 17 T was employed.

2. Synthesis of 3.

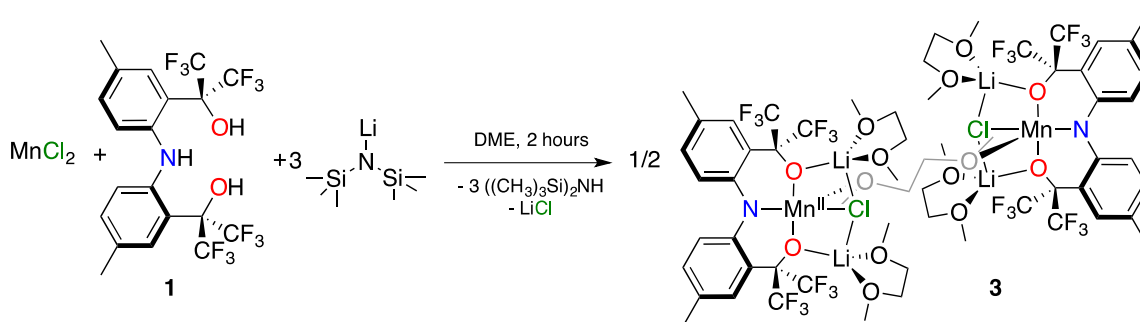


Figure S1. Synthesis of **3**.

Proligand **1** (0.200 g, 0.378 mmol) was dissolved in DME (1 mL) and three equivalents of $((\text{CH}_3)_3\text{Si})_2\text{NLi}$, 97 % (0.196 g, 1.136 mmol) in DME (1 mL) were added dropwise to generate the $[\text{CF}_3\text{-ONO}]\text{Li}_3$ species *in situ*. This solution was slowly added to a pink suspension of MnCl_2 , 99 % (0.058 g, 0.456 mmol) in DME (1 mL). Stirring this mixture for 2 hours yielded a brown solution. Filtering the reaction mixture through celite and removing all volatiles under vacuum produced a sticky brown oil, which is triturated 5 times with 2 mL of pentane to produce yellow powder. Dissolving this powder in Et_2O (5 mL) produced a white precipitate. This precipitate was filtered out and the resulting brown solution reduced under vacuum and triturated 5 times with 2 mL of pentane to produce an analytically pure yellow powder (0.279 g, 86.3 %). Cooling a concentrated Et_2O solution of **3** to $-35\text{ }^\circ\text{C}$ yielded yellow crystals suitable for X-ray analysis. $^1\text{H-NMR}$ (C_6D_6 , 300 MHz, $25\text{ }^\circ\text{C}$) δ (ppm): 33.17 ($\nu_{1/2} = 2700\text{ Hz}$), 25.12 ($\nu_{1/2} = 450\text{ Hz}$), 6.10 ($\nu_{1/2} = 1500\text{ Hz}$), and 0.11 ($\nu_{1/2} = 300\text{ Hz}$). Elemental analysis calcd. (%) for $\text{C}_{60}\text{H}_{74}\text{Cl}_2\text{F}_{24}\text{Mn}_2\text{Li}_4\text{N}_2\text{O}_{14}$ (1711.75 g/mol): C 42.10, H 4.36, and N 1.64; found: C 41.87, H 4.18, and N 1.92.

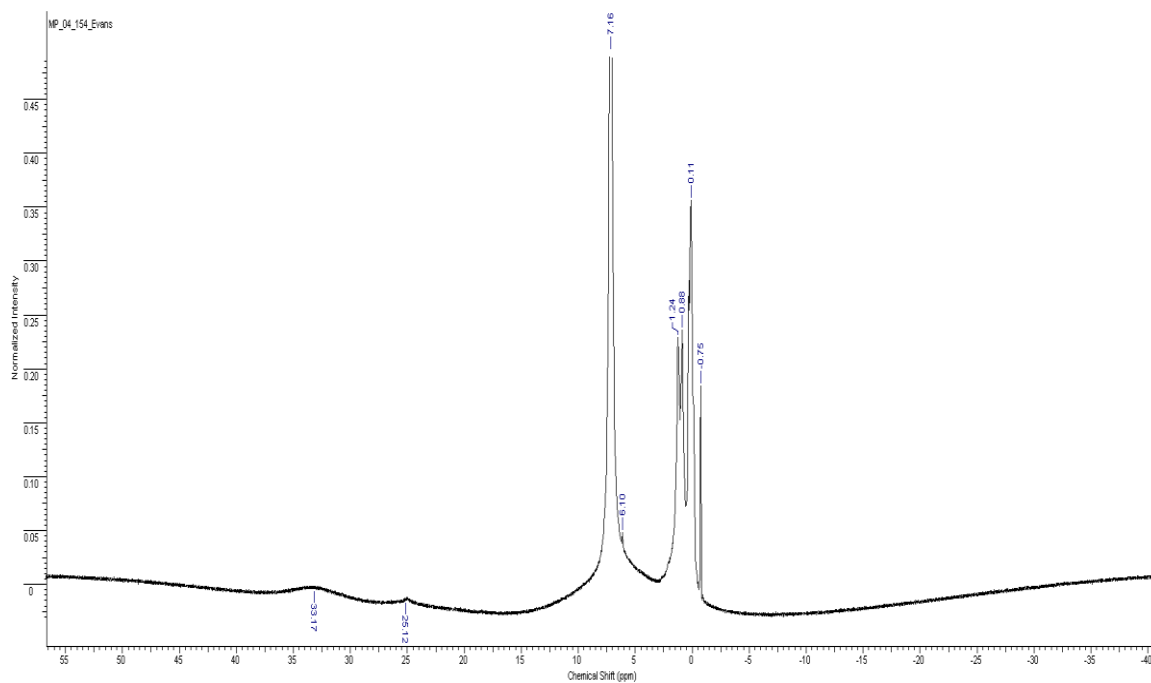


Figure S2. ^1H NMR spectrum of **3** in C_6D_6 .

3. X-ray crystallography of 3

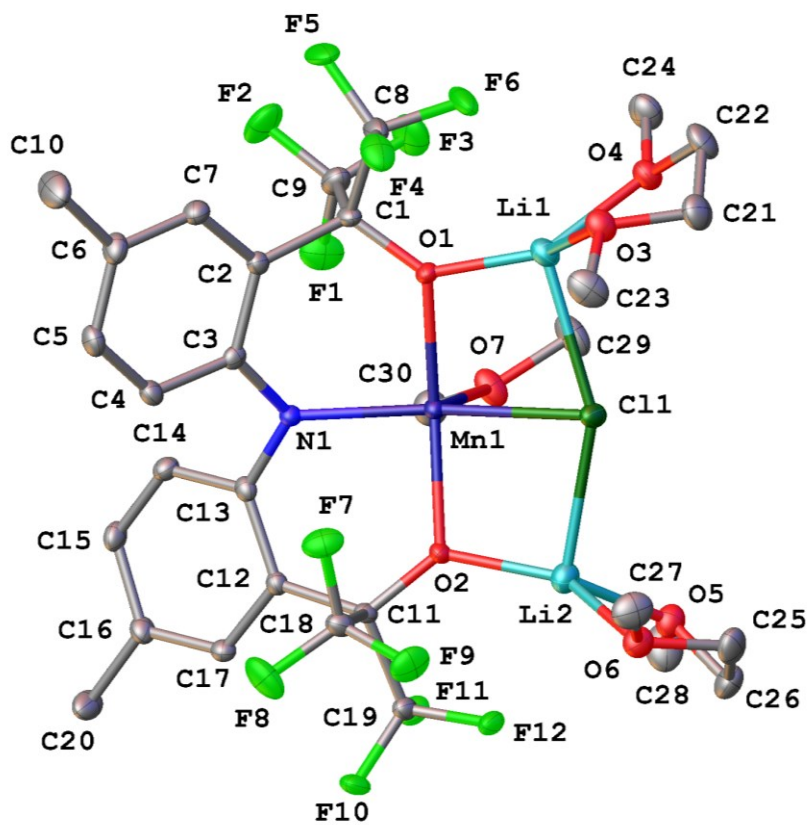


Figure S3. Molecular structure of **3**. Ellipsoids drawn at the 50 % probability level. Hydrogen atoms are omitted for clarity.

X-ray Experimental for 3.

X-Ray Intensity data were collected at 100 K on a Bruker **DUO** diffractometer using MoK radiation ($\lambda = 0.71073 \text{ \AA}$) and an APEXII CCD area detector.

Raw data frames were read by program SAINT and integrated using 3D profiling algorithms. The resulting data were reduced to produce hkl reflections and their intensities and estimated standard deviations. The data were corrected for Lorentz and polarization effects and numerical absorption corrections were applied based on indexed and measured faces.

The structure was solved and refined in SHELXTL2013, using full-matrix least-squares refinement. The non-H atoms were refined with anisotropic thermal parameters and all of the H atoms were calculated in idealized positions and refined riding on their parent atoms. The dimers are located in inversion centers with the linking ligand being a DME where C30 connects to its symmetry equivalent. In the final cycle of refinement, 8637 reflections (of which 6608 are observed with $I > 2\sigma(I)$) were used to refine 494 parameters and the resulting R_1 , wR_2 and S (goodness of fit) were 3.20%, 7.58% and 0.975, respectively. The refinement was carried out by minimizing the wR_2 function using F^2 rather than F values. R_1 is calculated to provide a reference to the conventional R value but its function is not minimized.

Table S1. Crystal data and structure refinement for **3**.

Identification code	pasc30	
Empirical formula	$C_{60}H_{74}Cl_2F_{24}Li_4Mn_2N_2O_{14}$	
Formula weight	1711.75	
Temperature	100(2) K	
Wavelength	0.71073 Å	
Crystal system	Triclinic	
Space group	P -1	
Unit cell dimensions	a = 11.7492(6) Å	$\alpha = 66.5970(11)^\circ$
	b = 12.6849(7) Å	$\beta = 72.1457(11)^\circ$
	c = 15.5600(8) Å	$\gamma = 63.4597(10)^\circ$
Volume	1880.28(17) Å ³	
Z	1	
Density (calculated)	1.512 Mg/m ³	
Absorption coefficient	0.525 mm ⁻¹	
F(000)	872	
Crystal size	0.140 x 0.132 x 0.031 mm ³	
Theta range for data collection	1.444 to 27.500°	
Index ranges	-15 ≤ h ≤ 13, -16 ≤ k ≤ 16, -20 ≤ l ≤ 20	
Reflections collected	30339	
Independent reflections	8637 [R(int) = 0.0331]	
Completeness to theta = 25.242°	100.0 %	
Absorption correction	Analytical	
Max. and min. transmission	0.9877 and 0.9425	
Refinement method	Full-matrix least-squares on F ²	
Data / restraints / parameters	8637 / 0 / 494	
Goodness-of-fit on F ²	0.975	
Final R indices [I > 2σ(I)]	R1 = 0.0320, wR2 = 0.0758 [6608]	
R indices (all data)	R1 = 0.0482, wR2 = 0.0798	
Extinction coefficient	n/a	
Largest diff. peak and hole	0.552 and -0.435 e.Å ⁻³	

$$R1 = \frac{\sum(|F_o| - |F_c|)}{\sum F_o}$$

$$wR2 = \frac{[\sum[w(F_o^2 - F_c^2)^2]]}{\sum[w(F_o^2)^2]}^{1/2}$$

$$S = [\sum[w(F_o^2 - F_c^2)^2] / (n-p)]^{1/2}$$

$$w = 1/[\sigma^2(F_o^2) + (m*p)^2 + n*p], p = [\max(F_o^2, 0) + 2*F_c^2]/3, m \& n \text{ are constants.}$$

4. Synthesis of 4.

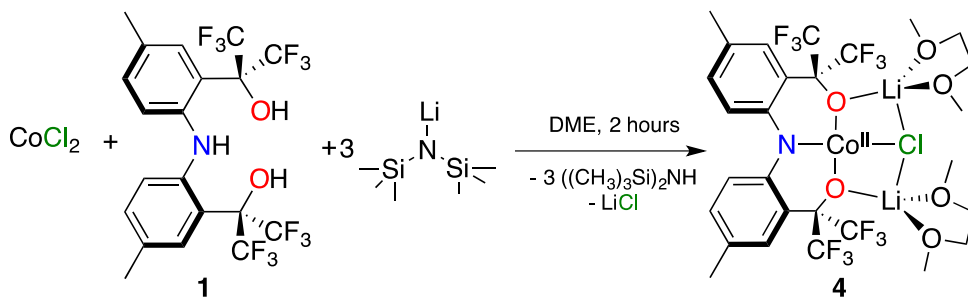


Figure S4. Synthesis of 4.

Proligand **1** (0.200 g, 0.378 mmol) was dissolved in DME (1 mL) and three equivalents of $((\text{CH}_3)_3\text{Si})_2\text{NLi}$, 97 % (0.196 g, 1.136 mmol) in DME (1 mL) were added dropwise to generate the $[\text{CF}_3\text{-ONO}]\text{Li}_3$ species *in situ*. This solution was slowly added to a light blue suspension of CoCl_2 , 99 % (0.050 g, 0.381 mmol) in DME (1 mL). Stirring this mixture for 2 hours yielded a red-brown solution. Filtering the reaction mixture through celite and removing all volatiles under vacuum produced a brown oil, which is triturated 5 times with 2 mL of pentane to produce an orange powder. This powder was washed 3 times with 5 mL of a pentane/DME (9:1) solution and 3 times with 5 mL of pentane. The remaining powder was dissolved in 20 mL of Et_2O and filtered through a celite pad to remove copious amounts of insoluble inorganic salts. After removing all volatiles under vacuum an analytically pure orange powder was obtained (0.144 g, 46.8 %). Cooling a concentrated Et_2O solution of **4** to $-35\text{ }^\circ\text{C}$ yielded red crystals suitable for X-ray analysis. $^1\text{H-NMR}$ (C_6D_6 , 300 MHz, $25\text{ }^\circ\text{C}$) δ (ppm): 52.99 ($\nu_{1/2} = 90\text{ Hz}$), 46.57 ($\nu_{1/2} = 90\text{ Hz}$), 46.17 ($\nu_{1/2} = 90\text{ Hz}$), 10.78 ($\nu_{1/2} = 600\text{ Hz}$), 3.19 ($\nu_{1/2} = 90\text{ Hz}$), 1.04 ($\nu_{1/2} = 150\text{ Hz}$), -7.59 ($\nu_{1/2} = 390\text{ Hz}$), and -12.81 ($\nu_{1/2} = 120\text{ Hz}$). Elemental analysis calcd. (%) for $\text{C}_{28}\text{H}_{32}\text{ClF}_{12}\text{CoLi}_2\text{NO}_6$ (814.81 g/mol): C 41.27, H 3.96, and N 1.72; found: C 41.10, H 3.85, and N 1.76.

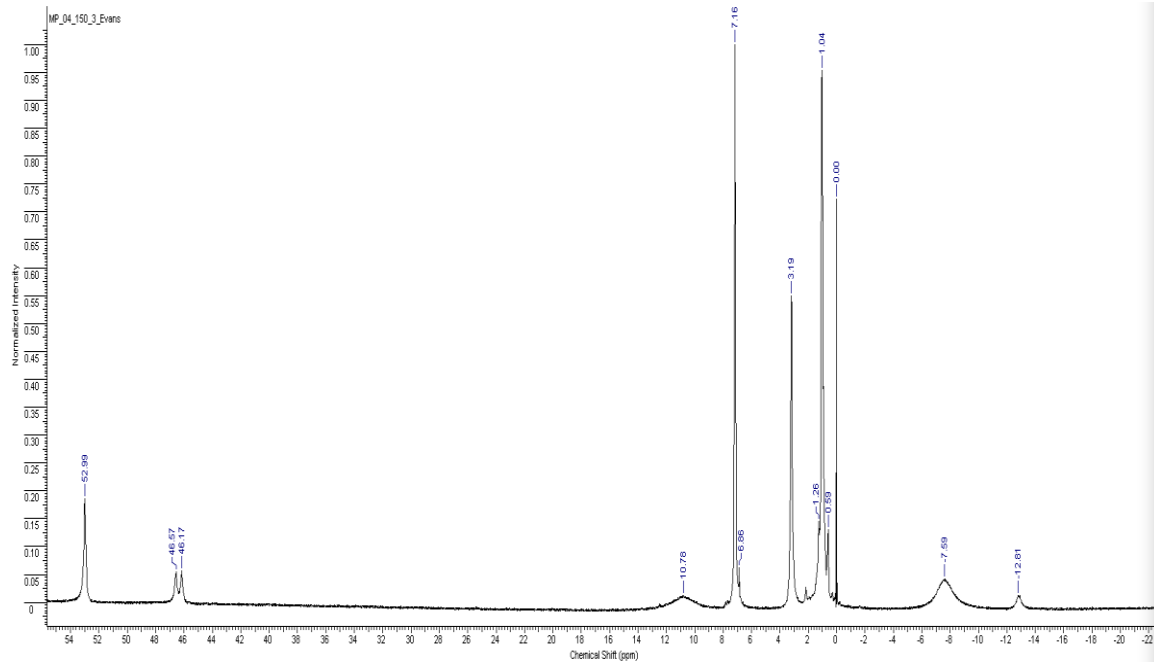


Figure S5. ^1H NMR spectrum of **4** in C_6D_6

5. X-ray crystallography of 4.

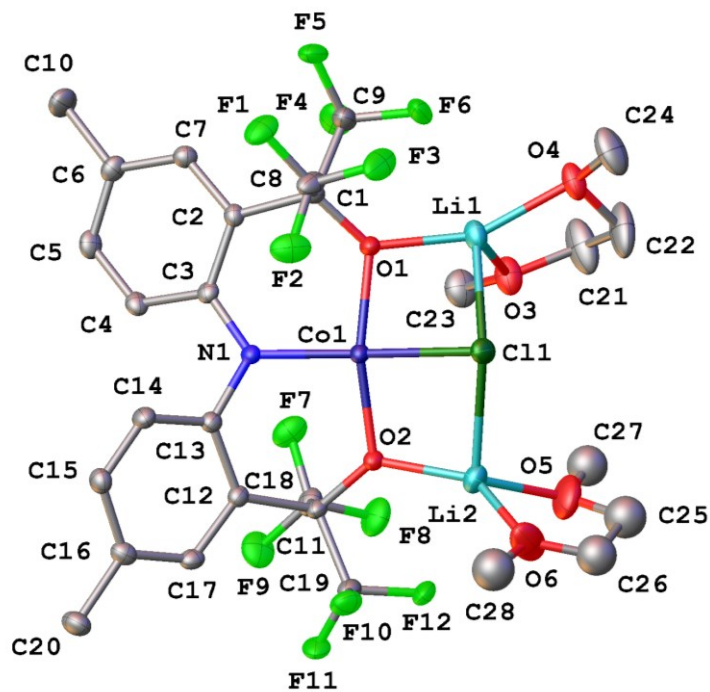


Figure S6. Molecular structure of 4. Ellipsoids shown at the 50 % probability level. Hydrogen atoms are omitted for clarity

X-ray Experimental for 4.

X-Ray Intensity data were collected at 100 K on a Bruker **DUO** diffractometer using MoK α radiation ($\lambda = 0.71073 \text{ \AA}$) and an APEXII CCD area detector.

Raw data frames were read by program SAINT and integrated using 3D profiling algorithms. The resulting data were reduced to produce hkl reflections and their intensities and estimated standard deviations. The data were corrected for Lorentz and polarization effects and numerical absorption corrections were applied based on indexed and measured faces.

The structure was solved and refined in SHELXTL2013, using full-matrix least-squares refinement. The non-H atoms were refined with anisotropic thermal parameters and all of the H atoms were calculated in idealized positions and refined riding on their parent atoms. One DME ligand is disordered except for the coordinated oxygen atoms. Its carbon and hydrogen atoms were refined in two parts with their site occupation factors dependently refined. In the final cycle of refinement, 8024 reflections (of which 6014 are observed with $I > 2\sigma(I)$) were used to refine 465 parameters and the resulting R_1 , wR_2 and S (goodness of fit) were 3.66%, 8.88% and 1.044, respectively. The refinement was carried out by minimizing the wR_2 function using F^2 rather than F values. R_1 is calculated to provide a reference to the conventional R value but its function is not minimized.

Table S2. Crystal data and structure refinement for **4**.

Identification code	pasc29	
Empirical formula	$C_{28}H_{32}ClCoF_{12}Li_2NO_6$	
Formula weight	814.80	
Temperature	100(2) K	
Wavelength	0.71073 Å	
Crystal system	Monoclinic	
Space group	$P 2_1/n$	
Unit cell dimensions	$a = 13.7122(14)$ Å	$\alpha = 90^\circ$
	$b = 14.9092(15)$ Å	$\beta = 98.473(2)^\circ$
	$c = 17.2336(18)$ Å	$\gamma = 90^\circ$
Volume	$3484.8(6)$ Å ³	
Z	4	
Density (calculated)	1.553 Mg/m ³	
Absorption coefficient	0.673 mm ⁻¹	
F(000)	1652	
Crystal size	0.232 x 0.192 x 0.038 mm ³	
Theta range for data collection	1.776 to 27.497°	
Index ranges	$-17 \leq h \leq 17, -19 \leq k \leq 19, -21 \leq l \leq 22$	
Reflections collected	48152	
Independent reflections	8024 [R(int) = 0.0438]	
Completeness to theta = 25.242°	100.0 %	
Absorption correction	Analytical	
Max. and min. transmission	0.9776 and 0.9055	
Refinement method	Full-matrix least-squares on F ²	
Data / restraints / parameters	8024 / 0 / 465	
Goodness-of-fit on F ²	1.044	
Final R indices [I > 2σ(I)]	R1 = 0.0366, wR2 = 0.0888 [6014]	
R indices (all data)	R1 = 0.0551, wR2 = 0.0941	
Extinction coefficient	n/a	
Largest diff. peak and hole	0.837 and -0.602 e.Å ⁻³	

$$R1 = \frac{\sum(|F_o| - |F_c|)}{\sum F_o}$$

$$wR2 = \frac{[\sum(w(F_o^2 - F_c^2)^2)]}{\sum[w(F_o^2)^2]}^{1/2}$$

$$S = [\sum(w(F_o^2 - F_c^2)^2) / (n-p)]^{1/2}$$

$$w = 1/[\sigma^2(F_o^2) + (m^*p)^2 + n^*p], p = [\max(F_o^2, 0) + 2 * F_c^2] / 3, m \text{ \& } n \text{ are constants.}$$

6. Synthesis of 5.

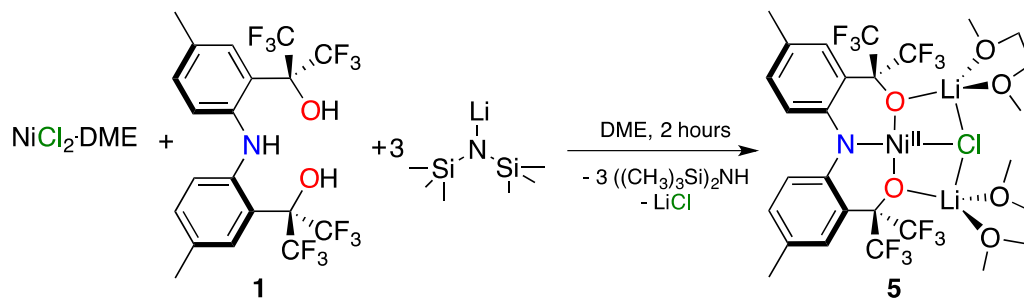


Figure S7. Synthesis of 5.

Proligand **1** (0.100 g, 0.189 mmol) was dissolved in DME (1 mL) and three equivalents of ((CH₃)₃Si)₂NLi, 97 % (0.098 g, 0.586 mmol) in DME (1 mL) were added dropwise to generate the [CF₃-ONO]Li₃ species *in situ*. This solution was slowly added to a yellow suspension of NiCl₂·DME, 97 % (0.043 g, 0.190 mmol) in DME (1 mL). Stirring this mixture for 2 hours yielded a green solution. Removal of all volatiles under vacuum produced a green powder, which is triturated 5 times with 2 mL of pentane. The powder was dissolved in 20 mL of Et₂O and filtered through a celite pad to remove copious amounts of insoluble inorganic salts. After removing all volatiles under vacuum, the solid is triturated 5 times with 2 mL of pentane to produce an analytically pure green powder (0.087 g, 56.5 %). Cooling a concentrated Et₂O solution of **5** to -35 °C yielded green crystals suitable for X-ray analysis. ¹H-NMR (C₆D₆, 300 MHz, 25 °C) δ (ppm): 7.55 (s, 2H, Ar-*H*), 7.49 (d, ³*J* = 9.00 Hz, 2H, Ar-*H*), 6.81 (d, ³*J* = 9.00 Hz, 2H, Ar-*H*), 3.45 (s, 12H, CH₃OCH₂CH₂OCH₃), 2.73 (s, 8H, CH₃OCH₂CH₂OCH₃), and 2.14 (s, 6H Ar-CH₃). ¹⁹F{¹H}-NMR (C₆D₆, 282 MHz, 25 °C) δ (ppm): -72.92 (q, ⁴*J* = 8.46 Hz, 6F), and -76.50 (q, ⁴*J* = 8.46 Hz, 6F). ¹³C{¹H}-NMR (C₆D₆, 126 MHz, 25 °C) δ (ppm): 131.02 (s, Ar C), 126.74 (s, Ar C), 125.84 (s, Ar C), 121.96 (s, Ar C), 70.29 (s, CH₃OCH₂CH₂OCH₃), 59.61 (s, CH₃OCH₂CH₂OCH₃), and 21.21 (s, Ar-CH₃). Elemental analysis calcd. (%) for

$C_{28}H_{32}ClF_{12}NiLi_2NO_6$ (814.57 g/mol): C 41.29, H 3.96, and N 1.72; found: C 41.27, H 3.96, and N 1.96.

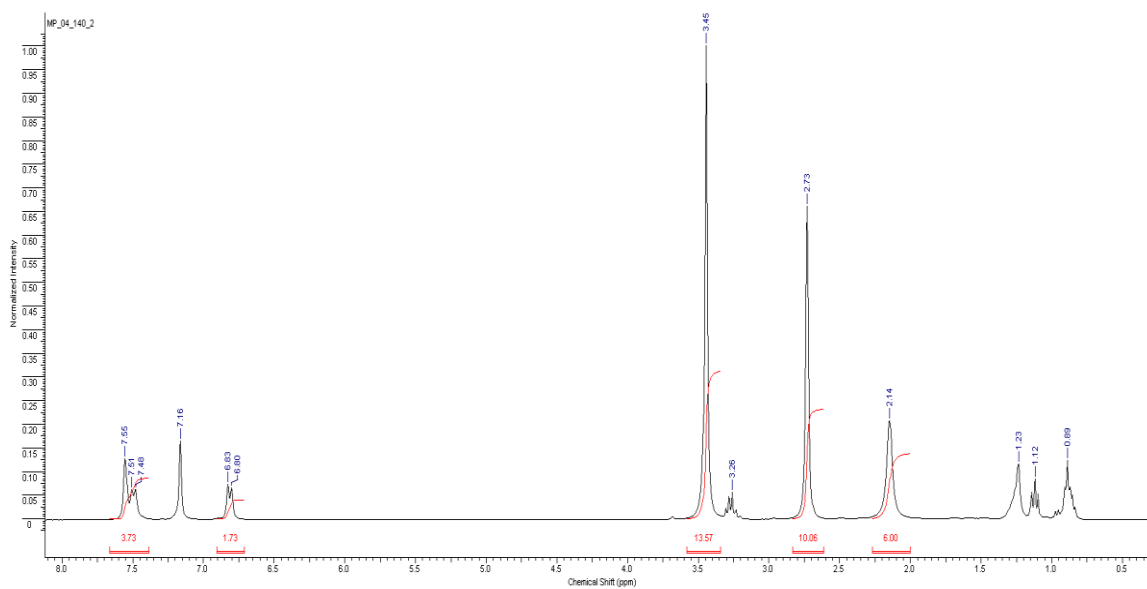


Figure S8. 1H NMR spectrum of **5** in C_6D_6 .

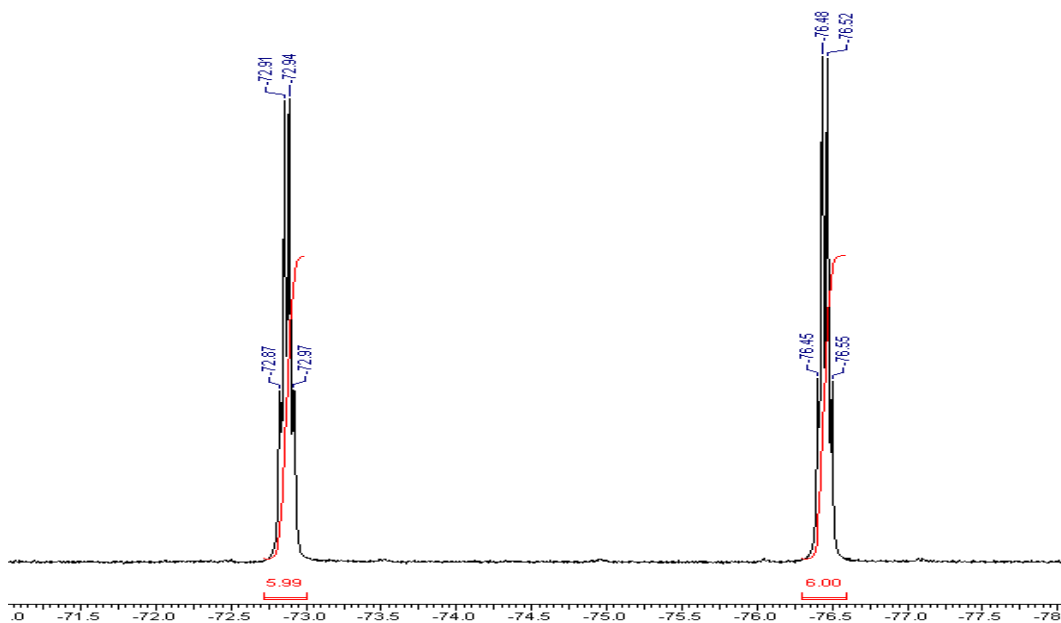


Figure S9. $^{19}F\{^1H\}$ NMR spectrum of **5** in C_6D_6 .

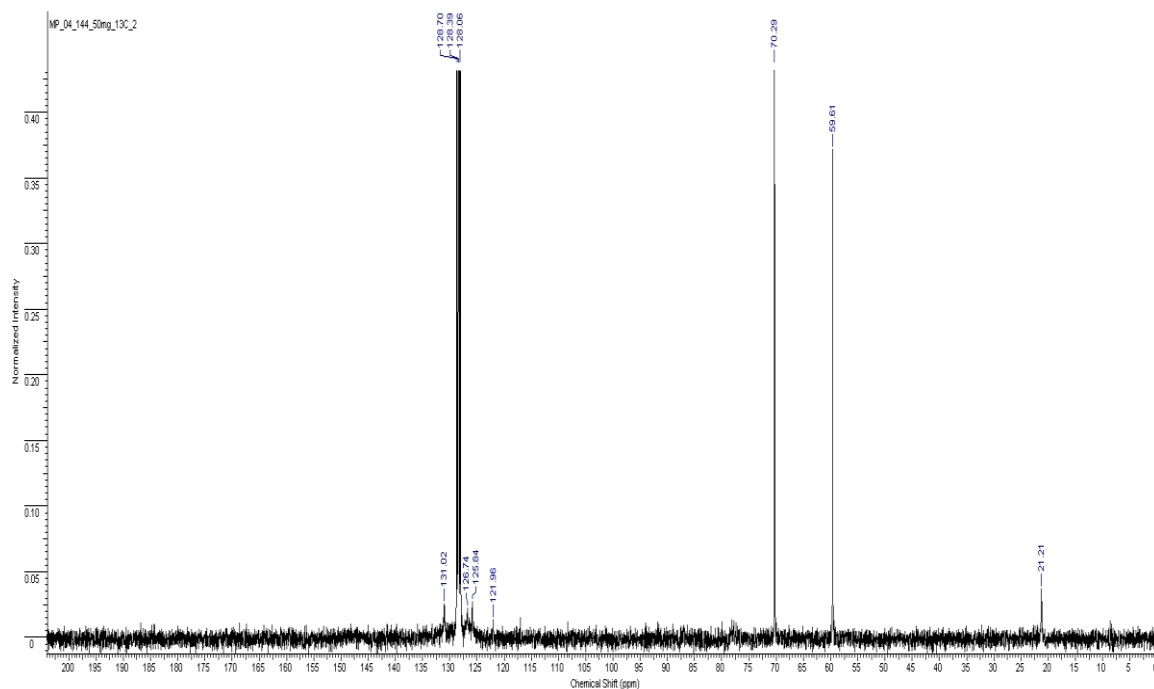


Figure S10. $^{13}\text{C}\{^1\text{H}\}$ NMR spectrum of **5** in C_6D_6 .

7. X-ray crystallography of 5.

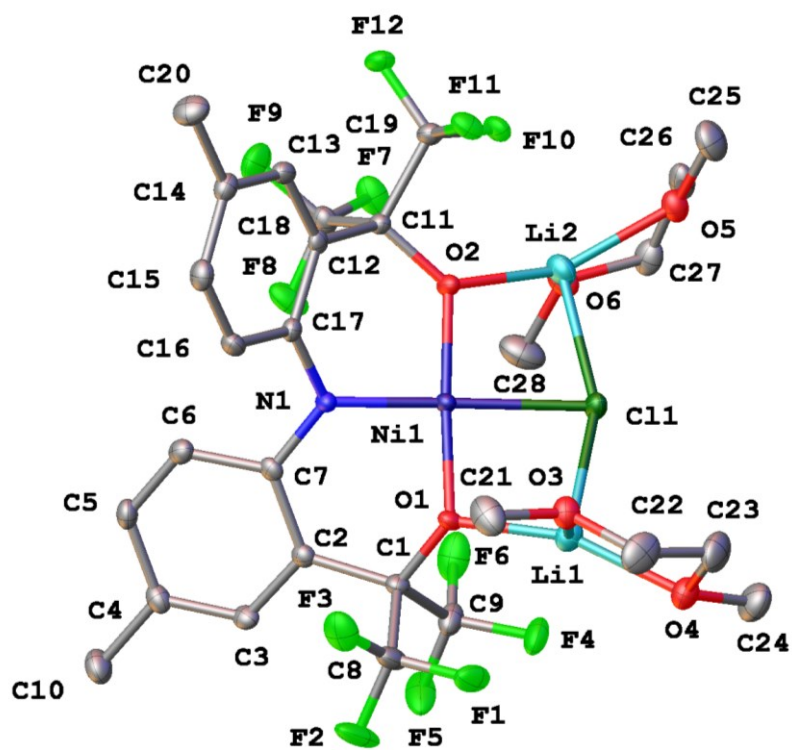


Figure S11. Molecular structure of **5**. Ellipsoids drawn at the 50 % probability level. Hydrogen atoms are omitted for clarity.

X-ray Experimental for 5.

Raw data frames were read by program SAINT and integrated using 3D profiling algorithms. The resulting data were reduced to produce hkl reflections and their intensities and estimated standard deviations. The data were corrected for Lorentz and polarization effects and numerical absorption corrections were applied based on indexed and measured faces.

The structure was solved and refined in SHELXTL2013, using full-matrix least-squares refinement. The non-H atoms were refined with anisotropic thermal parameters and all of the H atoms were calculated in idealized positions and refined riding on their parent atoms. There are two chemically equivalent but crystallographically independent Ni complexes in the asymmetric unit. In the final cycle of refinement, 15869 reflections (of which 10712 are observed with $I > 2\sigma(I)$) were used to refine 931 parameters and the resulting R_1 , wR_2 and S (goodness of fit) were 3.51%, 7.53% and 0.917, respectively. The refinement was carried out by minimizing the wR_2 function using F^2 rather than F values. R_1 is calculated to provide a reference to the conventional R value but its function is not minimized.

Table S3. Crystal data and structure refinement for **5**.

Identification code	pasc31	
Empirical formula	$C_{28}H_{32}ClF_{12}Li_2NNiO_6$	
Formula weight	814.58	
Temperature	100(2) K	
Wavelength	0.71073 Å	
Crystal system	Triclinic	
Space group	P -1	
Unit cell dimensions	a = 10.0895(7) Å	$\alpha = 84.244(1)^\circ$
	b = 11.9761(8) Å	$\beta = 87.334(1)^\circ$
	c = 30.403(2) Å	$\gamma = 70.942(1)^\circ$
Volume	3454.4(4) Å ³	
Z	4	
Density (calculated)	1.566 Mg/m ³	
Absorption coefficient	0.744 mm ⁻¹	
F(000)	1656	
Crystal size	0.21 x 0.057 x 0.056 mm ³	
Theta range for data collection	1.346 to 27.500°	
Index ranges	-12 ≤ h ≤ 13, -15 ≤ k ≤ 15, -39 ≤ l ≤ 39	
Reflections collected	58080	
Independent reflections	15869 [R(int) = 0.0463]	
Completeness to theta = 25.242°	100.0 %	
Absorption correction	Analytical	
Max. and min. transmission	0.9866 and 0.9163	
Refinement method	Full-matrix least-squares on F ²	
Data / restraints / parameters	15869 / 0 / 931	
Goodness-of-fit on F ²	0.917	
Final R indices [I > 2σ(I)]	R1 = 0.0351, wR2 = 0.0753 [10712]	
R indices (all data)	R1 = 0.0655, wR2 = 0.0854	
Extinction coefficient	n/a	
Largest diff. peak and hole	0.736 and -0.455 e.Å ⁻³	

$$R1 = \frac{\sum(|F_o| - |F_c|)}{\sum F_o}$$

$$wR2 = \frac{[\sum[w(F_o^2 - F_c^2)^2]]}{\sum[w(F_o^2)^2]}^{1/2}$$

$$S = [\sum[w(F_o^2 - F_c^2)^2] / (n-p)]^{1/2}$$

$$w = 1/[\sigma^2(F_o^2) + (m*p)^2 + n*p], p = [\max(F_o^2, 0) + 2*F_c^2]/3, m \text{ \& } n \text{ are constants.}$$

8. Magnetism Studies of 3 and 4.

Variable-temperature dc magnetic susceptibility data for microcrystalline powder samples of **3** and **4** in an applied field of 0.1 T were collected in the 5.0 – 300 K range using a Quantum Design MPMS-XL SQUID magnetometer equipped with a 7 T dc magnet. The sample was restrained in eicosane to prevent torquing. Diamagnetic corrections using Pascal's constants were applied to the observed susceptibilities to obtain the molar paramagnetic susceptibility (χ_M).

Figure S12 depicts the plot of $\chi_M T$ vs T for complex **4**. $\chi_M T$ steadily decreases with decreasing temperature from 2.83 cm³ mol⁻¹ K at 300 K to 1.33 cm³ mol⁻¹ K at 5.0 K. The 300 K value is much higher than the expected spin-only ($g = 2$) value of 1.875 cm³ mol⁻¹ K for a high-spin square-planar Co^{II} complex, which can be attributed to the presence of significant spin-orbit coupling effects. These values are consistent with values reported for other square-planar high-spin Co^{II} complexes.¹

Figure S13 depicts the plot of $\chi_M T$ vs T for complex **3**. $\chi_M T$ steadily decreases with decreasing temperature from 8.92 cm³ mol⁻¹ K at 300 K to 4.85 cm³ mol⁻¹ K at 5.0 K. The value at 300 K is in good agreement with the spin-only ($g = 2.00$) value, 8.75 cm³ K mol⁻¹, expected for two non-interacting high-spin Mn^{II} ions. Attempts to fit the data for D and g values yielded no acceptable fits.

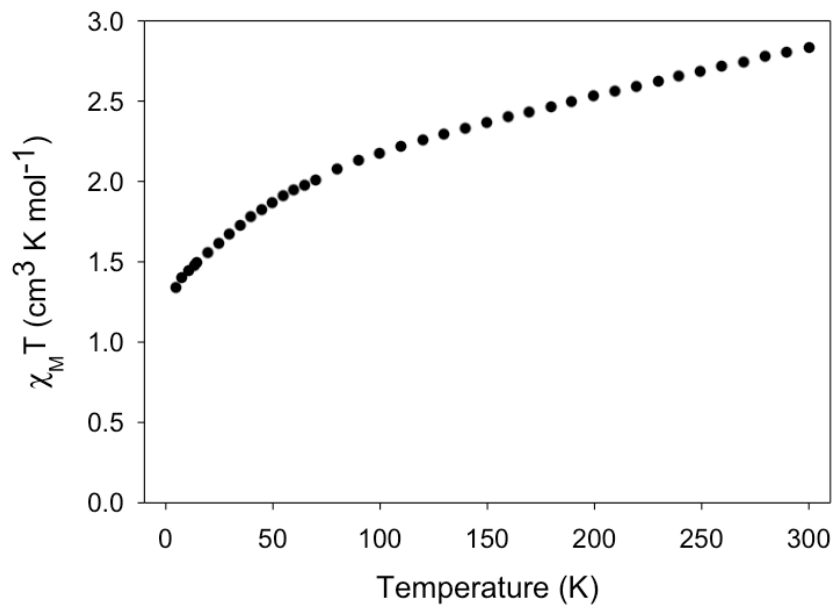


Figure S12. Temperature dependence of $\chi_M T$ for **4** measured using an applied field of 0.1 T.

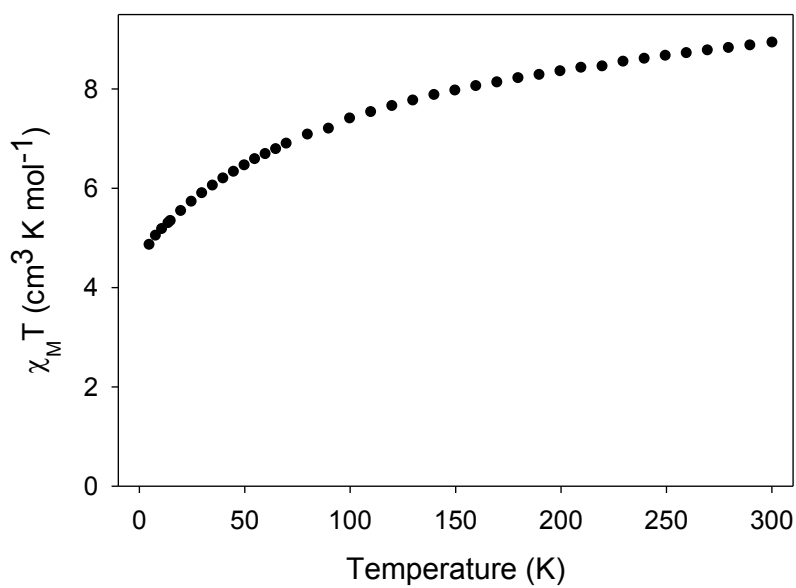


Figure S13. Temperature dependence of $\chi_M T$ for **3** measured using an applied field of 0.1 T.

9. DFT Calculations of **4**.

The DFT calculations were performed on two structural models of **4**, see Figure S14. We have assessed the relative energies of the lowest $M_S = 3/2$ and $M_S = 1/2$ states and found that as expected, the former is lower in energy, see Table S4. The expectation values of the \hat{S}^2 -spin operator, $\langle \hat{S}^2 \rangle \cong 3.7$, indicate that our DFT solutions are almost pure $S = 3/2$ states. In contrast the $\langle \hat{S}^2 \rangle \cong 0.9$ value obtained for the $M_S = 1/2$ states is considerably higher than that expected for a $S = 1/2$ spin state i.e., $\langle \hat{S}^2 \rangle \cong 0.75$. This value suggests that the latter states are multi-determinantal in nature which makes them difficult to describe in the framework of conventional DFT.

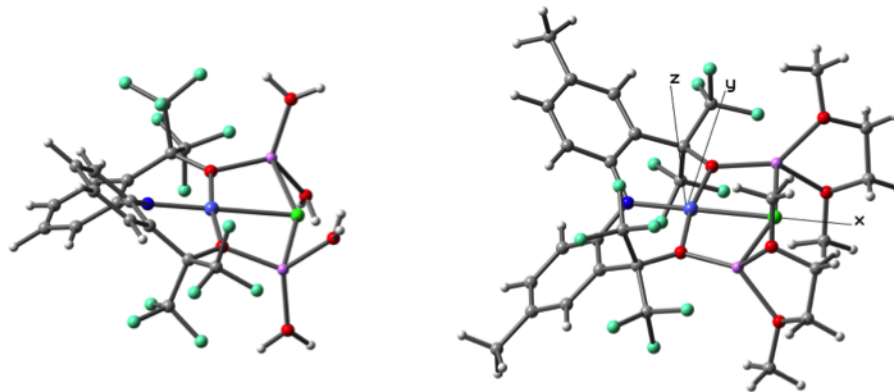


Figure S14. Structural models used for DFT. While the figure on the right was obtained starting from the geometry-optimized structure of the simplified model with a C_2 point group symmetry, that on the left was obtained from the geometry-optimized full, non-symmetrized model optimized (C_1 point group). The axes shown for the latter model indicate the frame used for the orbital labels below.

Table S4. Relative SCF Energies of the lowest quartet and doublet states obtained for the C_2 symmetrized and the non-symmetrized geometries of the full structural model of **4**.

Spin	Point Group Symmetry	Relative SCF Energies [cm^{-1}]	$\langle \hat{S}^2 \rangle$
3/2	C_1	0	3.757
	C_2	68	3.757
1/2	C_1	3245	0.921
	C_2	3259	0.916

Inspection of the predicted bond lengths and bond angles obtained from the geometry optimized structures reveals a good agreement between the experimental X-ray and the theoretical structures, see Table S5. Interestingly, both the experimental structure and those predicted for the non-symmetrized theoretical models reveal the presence of an approximate symmetry with a C_2 point group for which the two-fold rotation axis aligned with the N-Co-Cl moiety. This observation is further corroborated by the close SCF energies predicted for the symmetrized and non-symmetrized models. This suggests that the g and ZFS tensors share a common axis which is expected to be parallel to the Co-Cl and Co-N bonds. Finally, in order to test the effects that the peripheral substituents have on the electronic structure of the iron site we have also investigated a truncated computational model, see Figure S14. These calculations revealed that as expected, the Li-bound solvent molecules and the peripheral Me- groups of the ONO^{3-} ligand have essentially no bearing on the electronic structure of the $[CoO_2CIN]$ chromophore.

Table S5. Selected bond lengths and bond angles obtained from the geometry optimized and experimental structures.

	Full				Simplified	Exp.
	S = 1/2		S = 3/2		S = 3/2	
	C ₁	C ₂	C ₁	C ₂	C ₂	
Co-Cl	2.423	2.419	2.534	2.537	2.579	2.534
Co-N	1.853	1.853	1.906	1.853	1.911	1.906
Co-O	1.918 ^a	1.917	1.964 ^a	1.964	1.958	1.964 ^a
ClCoN	179.99	180	179.99	180	180	179.96
ClCoO	85.38 ^a	85.49	85.08 ^a	85.11	85.66	85.09 ^a
OCoN	94.61	94.5	94.91	94.88	94.33	94.91

a) Average values.

Crystal-Field Analysis of 4

The ground state character of the lowest quartet state was established on the basis of time-dependent (TD) DFT calculations. This state is best described as $|(xy)^2(z^2)^2(xy)^+(xz)^+(x^2-y^2)^+|$ and corresponds to a d^7 configuration for which the (xy) and

(z^2) orbitals are doubly occupied. Moreover, the (yz), (xz) and (x^2-y^2) orbitals are singly occupied and each accommodates a spin-up, alpha electron denoted by the “+” superscript. For this reference state the values of all excitations energies are positive. The stabilization of this ground state can be easily rationalized on the basis of the non-bonding character of the two doubly-occupied orbitals as well as on the basis of the small inter-electronic repulsions expected for this state, see Table S8. The assignment of the individual one-electron excitations and the values of their associated energies, as determined from the analysis of the TD-DFT calculations, are listed in **Table S6**. Inspection of this table reveals that all six d - d transitions expected for this configuration can be identified and are found among the lowest ten excitations. Surprisingly, the four lowest excitations are expressed in terms of two distinct components or individual transitions and involve the same set of donor and acceptor beta orbital pairs that is, $\{xy, z^2 \rightarrow yz, xz\}$. This observation suggests that the four lowest excited orbital states cannot be expressed in terms of a single determinant function and that in fact they are represented by a linear combination of configurations each one involving two of the $\{xy, xz, yz, z^2\}$ set of doubly occupied orbitals.

Table S6. Energies and assignments of the ten lowest excitations predicted using B3LYP/6-311G for the quartet ground state configuration.

#	Assignment	C ₁ full		C ₂ simplified		
		Energy [cm ⁻¹]	$\langle \hat{S}^2 \rangle$	Energy [cm ⁻¹]	Sym.	$\langle \hat{S}^2 \rangle$
1	$\{z^2 \rightarrow xz\}$ $\{xy \rightarrow yz\}$	3955	3.755	3668	B	3.755
2	$\{z^2 \rightarrow yz\}$ $\{xy \rightarrow zz\}$	4216	3.755	4118	A	3.755
3	$\{z^2 \rightarrow yz\}$ $\{xy \rightarrow xz\}$	9926	3.757	9711	A	3.757
4	$\{z^2 \rightarrow xz\}$ $\{xy \rightarrow yz\}$	10092	3.756	9559	B	3.759
5	$\{xy \rightarrow x^2-y^2\}$	17070	3.758	16873	B	3.759
6	$\{ligand \rightarrow xz\}$	19585	3.830	19778	A	3.816
7	$\{ligand \rightarrow yz\}$	19723	3.790	20119	B	3.790
8	$\{ligand \rightarrow ligand\}$	23738	5.472	24288	B	5.430
9	$\{z^2 \rightarrow x^2-y^2\}$	25579	3.773	25134	A	3.766
10	$\{ligand \rightarrow ligand\}$	25941	5.503	26328	B	5.479

A series of single-point calculations provide further insight into the nature of the four lowest orbital states. These calculations employ the geometry-optimized structure obtained for the $|(xy)^2(z^2)^2(xy)^+(xz)^+(x^2-y^2)^+|$ configuration combined with carefully prepared initial electronic guesses obtained from a set of suitable alterations, providing approximate SCF-DFT energies of a subset of quartet states. The nature of the electronic configuration corresponding to each of these Kohn-Sham states was established by investigating the gross orbital populations, see

Table S7.

Table S7. Relative SCF-energies of quartet states and their assignment on the basis of the gross orbital population.

State ^a	Rel. En. [cm ⁻¹]	$\langle \hat{S}^2 \rangle$	Total					Spin				
			z^2	yz	xz	x^2-y^2	xy	z^2	yz	xz	x^2-y^2	xy
$(xy)(z^2)$	0	3.757	1.879	1.155	1.056	1.19	1.899	0.035	0.831	0.938	0.811	0.063
$(xz)(yz+xy)$	4695	3.757	1.159	1.589	1.77	1.213	1.49	0.755	0.395	0.22	0.786	0.474
$(yz)(xy)$	5720	3.755	1.005	1.978	1.059	1.188	1.951	0.925	0.004	0.936	0.814	0.01
$(z^2)(xz)$	5593	3.76	1.791	1.071	1.974	1.302	1.036	0.117	0.915	0.016	0.702	0.935
$(z^2)(x^2-y^2)$	14189	3.757	1.871	1.129	1.081	1.985	1.024	0.049	0.858	0.914	0.013	0.946
$(yz)(xz)$	4863	3.754	1.057	1.976	1.912	1.223	1.029	0.859	0.006	0.079	0.781	0.942

a) Only the doubly occupied orbitals are indicated.

The energies of the ten quartet states can be expressed as a function of the Racah parameters (A, B, and C), which describe the inter-electronic repulsion of the 3d electrons. Then, the energies of the d - d transitions involving the $|(xy)^2(z^2)^2(xy)^+(xz)^+(x^2-y^2)^+|$ ground orbital state can be evaluated as function of the orbital energies (ϵ_i) of the 3d orbitals, and of the Racah parameter B (Table S8). The energies of the d - d transitions are independent of the choice of origin and thus of A and C.

Table S8. Expressions of the interelectronic repulsions and of the d-d transitions energies involving the $|(xy)^2(z^2)^2(xy)^+(xz)^+(x^2-y^2)^+|$ ground state configuration.

State ^a	d – d transition	Interelectronic Repulsion	Transition Energies	Transition Energies [cm ⁻¹] ^c
$(xy)(z^2)$	n.a.	21A-43B+14C	0	0
$(z^2)(xz)$	$\{xy \rightarrow xz\}^d$	21A-34B+14C	$9B+\varepsilon(xz)-\varepsilon(xy)$	5593
$(z^2)(yz)$	$\{xy \rightarrow yz\}^d$	21A-34B+14C	$9B+\varepsilon(yz)-\varepsilon(xy)$	-
$(z^2)(x^2-y^2)$	$\{xy \rightarrow x^2-y^2\}^d$	21A-43B+14C	$\varepsilon(x^2-y^2)-\varepsilon(xy)$	14189/17070
$(xy)(xz)$	$\{z^2 \rightarrow xz\}^d$	21A-40B+14C	$3B+\varepsilon(xz)-\varepsilon(z^2)$	4527^b
$(xy)(yz)$	$\{z^2 \rightarrow yz\}^d$	21A-40B+14C	$3B+\varepsilon(yz)-\varepsilon(z^2)$	5720
$(xy)(x^2-y^2)$	$\{z^2 \rightarrow x^2-y^2\}^d$	21A-31B+14C	$12B+\varepsilon(x^2-y^2)-\varepsilon(z^2)$	25580
$(xz)(yz)$	$\{xy, z^2 \rightarrow xz, yz\}^e$	21A-40B+14C	$3B+\varepsilon(xz)+\varepsilon(yz)-\varepsilon(xy)-\varepsilon(z^2)$	4863
$(xz)(x^2-y^2)$	$\{xy, z^2 \rightarrow xz, x^2-y^2\}^e$	21A-40B+14C	$3B+\varepsilon(xz)+\varepsilon(x^2-y^2)-\varepsilon(xy)-\varepsilon(z^2)$	-
$(yz)(x^2-y^2)$	$\{xy, z^2 \rightarrow yz, x^2-y^2\}^e$	21A-40B+14C	$3B+\varepsilon(yz)+\varepsilon(x^2-y^2)-\varepsilon(xy)-\varepsilon(z^2)$	-

- a) Only the doubly occupied orbitals are indicated.
b) Value derived from the relative SCF Energy of the $|(xz)(yz+xy)|$ state.
c) Table S7. Shown in black are values derived from the analysis of the TDDFT results presented in Table S6. Values determined for the C₁ full structural model. Shown in red are the values obtained from the relative SCF energies of the single point calculations.
d) Single electron excitations.
e) Two-electron excitations.

The crystal field energies ε_i and the Racah parameter B have been estimated using the least square fitting of TD-DFT excitation and the relative SCF energies of the quartet Kohn-Sham states using the theoretical expressions of Table S8. These values are listed in Table S9.

Table S9. Orbital energies determined from the CF analysis of the TDDFT and SCF energies.

Energies ^a	2	4	
	Fe ²⁺ , 3d ⁶	Co ²⁺ , 3d ⁷	
$\varepsilon(x^2-y^2)-\varepsilon(xy)$	14053	14189 ^c	17070 ^d
B	-	547	680
$\varepsilon(z^2)^b$	0	0	0
$\varepsilon(xy)$	3798	2115	3016
$\varepsilon(xz)$	5617	2752	2592 ^c

$\varepsilon(yz)$	6286	3811	3891
$\varepsilon(x^2-y^2)$	17851	19150	17310

- Values expressed in [cm^{-1}].
- Zero by definition.
- Value obtained from the relative SCF Energies.
- Value obtained from the TDDFT excitation energies.
- Although $\varepsilon(xz) < \varepsilon(xy)$ the $|(xy)^2(z^2)^2(xy)^+(xz)^+(x^2-y^2)^+|$ state is still the lowest in energy due to the small inter-electronic repulsions.

Table S10. Composition of the states with 4F parentage involving the any of the $\{xy, xz, yz, z^2\}$ doubly occupied orbitals.^{a, b}

	$(z^2)(xz)$	$(z^2)(yz)$	$(xy)(xz)$	$(xy)(yz)$	$(xz)(yz)$	$(xy)(x^2-y^2)$	$(xz)(x^2-y^2)$	$(yz)(x^2-y^2)$	Orbital Energies ^{c, d}	
$ ^4F, ES1\rangle$	1/2	0	0	$-\sqrt{3}/2$	0	0	0	0	5610	5510
$ ^4F, ES2\rangle$	0	1/2	$-\sqrt{3}/2$	0	0	0	0	0	4603	5179
$ ^4F, ES3\rangle$	1/2	0	0	0	0	0	$-\sqrt{3}/2$	0	17115	15575
$ ^4F, ES4\rangle$	0	1/2	0	0	0	0	0	$-\sqrt{3}/2$	18174	16874
$ ^4F, ES5\rangle$	0	0	0	0	$2/\sqrt{5}$	$1/\sqrt{5}$	0	0	9503	9252

- For clarity, we indicate only the doubly occupied orbitals.
- In addition to the functions listed here the ground state, $(xy)(z^2)$ ($|^4F, GS\rangle$), and the $(z^2)(x^2-y^2)$ excited state, ($|^4F, ES6\rangle$), configurations also belong to the 4F manifold.
- Values obtained using Table S9 and the reported relative to that of the $(xy)(z^2)$ ground state configuration expressed in [cm^{-1}].
- Values obtained for $\varepsilon(x^2-y^2) - \varepsilon(xy) = 14189(17070) \text{ cm}^{-1}$.

In order to evaluate the investigate the spin-orbit interaction we need to evaluate the matrix elements of the \hat{L}_ξ operators (where $\xi = x, y, z$) involving the $|(xy)^2(z^2)^2(xy)^+(xz)^+(x^2-y^2)^+|$ ground state and the first two excited states derived from the analysis of the TD DFT results. These numerical values of these parameters are listed in Table S11. Interestingly, values obtained for the $\{|(z^2), (xy)\rangle, |^4F, ES1\rangle, |^4F, ES2\rangle\}$ orbital states are identical to those involving the $\{|(z^2), (xy)\rangle, |(z^2), (yz)\rangle, |(z^2), (xz)\rangle\}$ configurations, see Table S11. Finally, these matrix elements have been used to evaluate the effective g values of the ground Kramers doublet. Thus, the plots of figure S15 were obtained by comparing the field dependence of the lowest energy levels as determined from the

diagonalization of the $\hat{\mathbf{H}} = \lambda \hat{\mathbf{L}} \cdot \hat{\mathbf{S}} + (\hat{\mathbf{L}} + 2\hat{\mathbf{S}})\vec{\mathbf{B}}$ Hamiltonian with those of a fictitious $S' = 1/2$

spin, $\hat{\mathbf{H}}_Z = \beta \hat{\mathbf{S}}' \cdot \tilde{\mathbf{g}} \cdot \vec{\mathbf{B}}$.

Table S11. Matrix elements of the \hat{L}_ξ (where $\xi = x, y, z$) operators of states involving the $\{xy, xz, yz, z^2\}$ orbital set.

\hat{L}_x		$ (z^2)(xy) $	$ (z^2)(xz) $	$ (z^2)(yz) $
		$ (z^2),(xy)\rangle$	$ ^4F,ES1\rangle$	$ ^4F,ES2\rangle$
$ (z^2)(xy) $	$ (z^2),(xy)\rangle$	0	i	0
$ (z^2)(xz) $	$ ^4F,ES1\rangle$	-i	0	0
$ (z^2)(yz) $	$ ^4F,ES2\rangle$	0	0	0

\hat{L}_y		$ (z^2)(xy) $	$ (z^2)(xz) $	$ (z^2)(yz) $
		$ (z^2),(xy)\rangle$	$ ^4F,ES1\rangle$	$ ^4F,ES2\rangle$
$ (z^2)(xy) $	$ (z^2),(xy)\rangle$	0	0	i
$ (z^2)(xz) $	$ ^4F,ES1\rangle$	0	0	0
$ (z^2)(yz) $	$ ^4F,ES2\rangle$	-i	0	0

\hat{L}_z		$ (z^2)(xy) $	$ (z^2)(xz) $	$ (z^2)(yz) $
		$ (z^2),(xy)\rangle$	$ ^4F,ES1\rangle$	$ ^4F,ES2\rangle$
$ (z^2)(xy) $	$ (z^2),(xy)\rangle$	0	0	0
$ (z^2)(xz) $	$ ^4F,ES1\rangle$	0	0	-i
$ (z^2)(yz) $	$ ^4F,ES2\rangle$	0	i	0

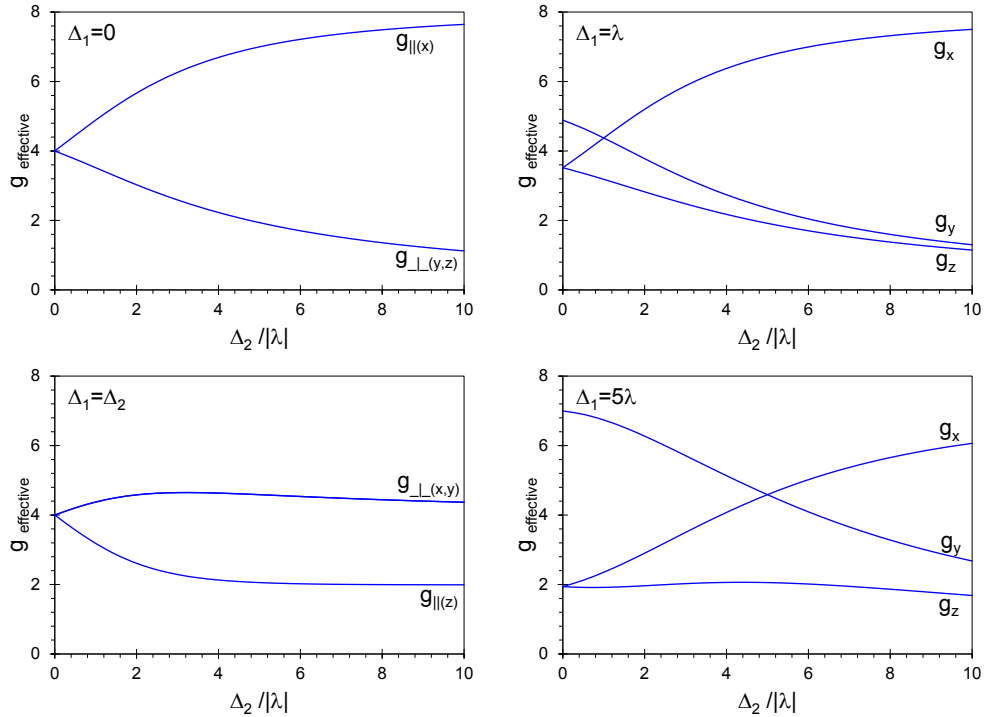


Figure S15. Effective g -values calculated for the ground Kramers doublet from the diagonalization of the $\hat{\mathbf{H}} = \lambda \hat{\mathbf{L}} \cdot \hat{\mathbf{S}} + (\hat{\mathbf{L}} + 2\hat{\mathbf{S}}) \vec{\mathbf{B}}$ Hamiltonian. The first term accounts for the spin-orbit coupling and the second for the Zeeman interactions. The $\langle i | \hat{\mathbf{L}}_{\xi} | j \rangle$ matrix elements are listed in Table S11, λ represents the spin-orbit coupling constant and $\Delta_{1,2}$ account for the energy separation between the orbital ground state and the first and second excited orbital state, respectively.

10. Effective g -values predicted for 4 using equation 1.

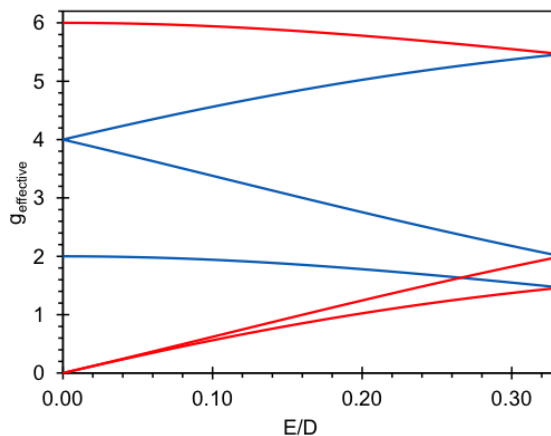


Figure S16. Effective g -values calculated in the low Zeeman field limit for the two Kramers doublets of a $S = 3/2$ spin system, using equation 1, as a function of the “rhombic” ZFS parameter E/D . The red traces correspond to the Kramers doublet which for $E/D \sim 0$ correspond to the $|\mathbf{S}, \mathbf{m}_s\rangle = |3/2, \pm 3/2\rangle$ levels and the blue to the $|\mathbf{S}, \mathbf{m}_s\rangle = |3/2, \pm 1/2\rangle$. Under these conditions the effective g -values are independent of D . These traces were calculated for $g_{x,y,z} = 2.00$.

11. Cartesian Coordinates of the Geometry Optimized Structures

S=3/2, C_2 point group, full structural model
E(UB3LYP) = -4648.87996038 A.U.

Co	0.00000	0.00000	0.14245
N	0.00000	0.00000	-1.76223
O	1.06709	1.64038	0.30972
Cl	0.00000	0.00000	2.67955
O	-1.06709	-1.64038	0.30972
C	1.08790	0.53275	-2.48043
C	-1.08790	-0.53275	-2.48043
C	1.46736	2.44777	-0.78258

Li	1.23717	2.07820	2.14527
Li	-1.23717	-2.07820	2.14527
C	-1.46736	-2.44777	-0.78258
C	1.82559	1.67900	-2.07088
C	1.52550	-0.12750	-3.65751
C	-1.82559	-1.67900	-2.07088
C	-1.52550	0.12750	-3.65751
C	2.69325	3.23611	-0.21696
C	0.32100	3.46625	-1.07042
O	0.28650	3.32490	3.35033
O	2.67836	2.11392	3.52765
O	-0.28650	-3.32490	3.35033
O	-2.67836	-2.11392	3.52765
C	-2.69325	-3.23611	-0.21696
C	-0.32100	-3.46625	-1.07042
C	2.88206	2.13572	-2.88398
C	2.58189	0.33250	-4.42162
H	1.00742	-1.02878	-3.94878
C	-2.88206	-2.13572	-2.88398
C	-2.58189	-0.33250	-4.42162
H	-1.00742	1.02878	-3.94878
F	2.43523	3.69700	1.09029
F	3.81608	2.42067	-0.09548
F	3.08618	4.37256	-0.92502
F	0.62510	4.35919	-2.09816
F	-0.85507	2.82115	-1.43223
F	0.00000	4.25014	0.05162
C	-1.16664	3.45285	3.28244
C	0.82098	3.06813	4.68177
C	2.32769	3.09050	4.55108
C	4.10809	1.93747	3.31466
C	-0.82098	-3.06813	4.68177
C	1.16664	-3.45285	3.28244
C	-4.10809	-1.93747	3.31466
C	-2.32769	-3.09050	4.55108
F	-2.43523	-3.69700	1.09029
F	-3.81608	-2.42067	-0.09548
F	-3.08618	-4.37256	-0.92502
F	0.00000	-4.25014	0.05162
F	-0.62510	-4.35919	-2.09816
F	0.85507	-2.82115	-1.43223
C	3.27858	1.49525	-4.05573
H	3.41726	3.03070	-2.61099

H	2.87645	-0.21634	-5.30863
C	-3.27858	-1.49525	-4.05573
H	-3.41726	-3.03070	-2.61099
H	-2.87645	0.21634	-5.30863
H	-1.64016	2.50472	3.54230
H	-1.39229	3.71552	2.25445
H	-1.50308	4.24939	3.94981
H	0.49159	3.84814	5.37492
H	0.47343	2.09266	5.03177
H	2.67567	4.08116	4.24498
H	2.79422	2.81946	5.50336
H	4.20906	1.20673	2.51948
H	4.58077	1.56390	4.22589
H	4.57181	2.87750	3.00885
H	-0.47343	-2.09266	5.03177
H	-0.49159	-3.84814	5.37492
H	1.50308	-4.24939	3.94981
H	1.64016	-2.50472	3.54230
H	1.39229	-3.71552	2.25445
H	-4.58077	-1.56390	4.22589
H	-4.57181	-2.87750	3.00885
H	-4.20906	-1.20673	2.51948
H	-2.67567	-4.08116	4.24498
H	-2.79422	-2.81946	5.50336
C	4.42171	2.02051	-4.89405
C	-4.42171	-2.02051	-4.89405
H	4.83554	2.93684	-4.47111
H	4.10149	2.24413	-5.91543
H	5.23557	1.29295	-4.96362
H	-4.83554	-2.93684	-4.47111
H	-4.10149	-2.24413	-5.91543
H	-5.23557	-1.29295	-4.96362

S=3/2, C₁ point group, full structural model
E(UB3LYP) = -4648.88027133 A.U.

Co	-0.00001	0.13710	0.00020
N	-0.00001	-1.76897	0.00011
O	-1.95318	0.30537	0.12252
Cl	0.00005	2.67119	0.00063
O	1.95314	0.30537	-0.12242
C	-1.08460	-2.48872	-0.53823
C	1.08461	-2.48875	0.53834
C	-2.83888	-0.78353	0.30693
Li	-2.41662	2.14024	0.19660

Li	2.41657	2.14027	-0.19632
C	2.83882	-0.78353	-0.30693
C	-2.44376	-2.08150	-0.42610
C	-0.82685	-3.66810	-1.28398
C	2.44376	-2.08152	0.42611
C	0.82692	-3.66813	1.28409
C	-4.20769	-0.22477	-0.20233
C	-2.95865	-1.04799	1.83987
O	-2.87082	3.40787	1.64887
O	-3.27672	3.48147	-1.00711
O	2.87037	3.40763	-1.64895
O	3.27717	3.48167	1.00686
C	4.20767	-0.22479	0.20224
C	2.95850	-1.04795	-1.83989
C	-3.44904	-2.90323	-0.97357
C	-1.83470	-4.43937	-1.83260
H	0.20391	-3.95650	-1.42515
C	3.44909	-2.90326	0.97349
C	1.83481	-4.43942	1.83261
H	-0.20384	-3.95652	1.42533
F	-4.41195	1.09446	0.25167
F	-4.24173	-0.13507	-1.59210
F	-5.35170	-0.91979	0.19173
F	-3.84480	-2.07898	2.15188
F	-1.73180	-1.38909	2.39552
F	-3.40210	0.08164	2.54991
C	-2.14009	3.38275	2.91280
C	-2.95121	4.71546	1.01001
C	-3.84849	4.54909	-0.19604
C	-3.97440	3.22728	-2.25997
C	2.95133	4.71532	-1.01039
C	2.13911	3.38242	-2.91258
C	3.97512	3.22758	2.25960
C	3.84897	4.54896	0.19539
F	4.41194	1.09442	-0.25182
F	4.24180	-0.13504	1.59200
F	5.35164	-0.91985	-0.19188
F	3.40186	0.08170	-2.54993
F	3.84467	-2.07891	-2.15197
F	1.73162	-1.38909	-2.39546
C	-3.18205	-4.07942	-1.67030
H	-4.48512	-2.63244	-0.84981
H	-1.57760	-5.32789	-2.39757

C	3.18214	-4.07946	1.67022
H	4.48516	-2.63247	0.84966
H	1.57776	-5.32794	2.39758
H	-1.09130	3.63318	2.74606
H	-2.22828	2.36770	3.28527
H	-2.59618	4.07773	3.62140
H	-3.38246	5.44525	1.70201
H	-1.94973	5.03617	0.71183
H	-4.86130	4.27189	0.10983
H	-3.88468	5.47895	-0.77230
H	-3.45760	2.40009	-2.73438
H	-3.93014	4.11073	-2.90098
H	-5.01400	2.95058	-2.07310
H	1.95004	5.03638	-0.71193
H	3.38255	5.44486	-1.70269
H	2.59498	4.07727	-3.62146
H	1.09041	3.63298	-2.74544
H	2.22705	2.36732	-3.28496
H	3.93123	4.11119	2.90042
H	5.01460	2.95058	2.07253
H	3.45822	2.40063	2.73433
H	4.86160	4.27141	-0.11077
H	3.88562	5.47892	0.77145
C	-4.29540	-4.92750	-2.24179
C	4.29554	-4.92755	2.24162
H	-5.27374	-4.50393	-2.01128
H	-4.27315	-5.94412	-1.83955
H	-4.21966	-5.00968	-3.32991
H	5.27386	-4.50401	2.01099
H	4.27322	-5.94418	1.83941
H	4.21991	-5.00970	3.32975

S = 1/2, C₂ point group, full structural model

E(UB3LYP) = -4648.86530521 A.U.

Co	0.00000	0.00000	0.14425
N	0.00000	0.00000	-1.70916
O	-0.04822	1.91119	0.29489
Cl	0.00000	0.00000	2.56389
O	0.04822	-1.91119	0.29489
C	0.64848	1.02059	-2.43017
C	-0.64848	-1.02059	-2.43017
C	-0.10265	2.82491	-0.78172
Li	-0.24457	2.39280	2.12238
Li	0.24457	-2.39280	2.12238

C	0.10265	-2.82491	-0.78172
C	0.65032	2.38373	-2.04324
C	1.38393	0.67851	-3.59355
C	-0.65032	-2.38373	-2.04324
C	-1.38393	-0.67851	-3.59355
C	0.50591	4.12959	-0.17637
C	-1.60338	3.09033	-1.12086
O	-1.84224	2.81228	3.20740
O	0.77506	3.21245	3.64282
O	1.84224	-2.81228	3.20740
O	-0.77506	-3.21245	3.64282
C	-0.50591	-4.12959	-0.17637
C	1.60338	-3.09033	-1.12086
C	1.31231	3.32923	-2.84992
C	2.04002	1.62518	-4.35878
H	1.43257	-0.36331	-3.87188
C	-1.31231	-3.32923	-2.84992
C	-2.04002	-1.62518	-4.35878
H	-1.43257	0.36331	-3.87188
F	0.00000	4.36377	1.12154
F	1.88361	4.02625	-0.01118
F	0.26497	5.31393	-0.87211
F	-1.77918	4.04001	-2.12941
F	-2.24649	1.93498	-1.54254
F	-2.33161	3.55564	-0.01142
C	-3.08750	2.07466	3.01462
C	-1.39150	2.90995	4.58940
C	-0.17058	3.80261	4.58104
C	2.05832	3.89476	3.55345
C	1.39150	-2.90995	4.58940
C	3.08750	-2.07466	3.01462
C	-2.05832	-3.89476	3.55345
C	0.17058	-3.80261	4.58104
F	0.00000	-4.36377	1.12154
F	-1.88361	-4.02625	-0.01118
F	-0.26497	-5.31393	-0.87211
F	2.33161	-3.55564	-0.01142
F	1.77918	-4.04001	-2.12941
F	2.24649	-1.93498	-1.54254
C	2.00746	2.98489	-4.00676
H	1.28037	4.37411	-2.58472
H	2.59309	1.30913	-5.23566
C	-2.00746	-2.98489	-4.00676

H	-1.28037	-4.37411	-2.58472
H	-2.59309	-1.30913	-5.23566
H	-2.95267	1.02811	3.29288
H	-3.31833	2.15470	1.95817
H	-3.88635	2.53038	3.60382
H	-2.17721	3.35144	5.21000
H	-1.14348	1.91340	4.96423
H	-0.43111	4.81265	4.25195
H	0.27170	3.84914	5.58111
H	2.63558	3.35747	2.80851
H	2.57121	3.86049	4.51735
H	1.92357	4.93076	3.23593
H	1.14348	-1.91340	4.96423
H	2.17721	-3.35144	5.21000
H	3.88635	-2.53038	3.60382
H	2.95267	-1.02811	3.29288
H	3.31833	-2.15470	1.95817
H	-2.57121	-3.86049	4.51735
H	-1.92357	-4.93076	3.23593
H	-2.63558	-3.35747	2.80851
H	0.43111	-4.81265	4.25195
H	-0.27170	-3.84914	5.58111
C	2.71024	4.02819	-4.84523
C	-2.71024	-4.02819	-4.84523
H	2.56273	5.02906	-4.43750
H	2.33988	4.03315	-5.87407
H	3.78795	3.84668	-4.89154
H	-2.56273	-5.02906	-4.43750
H	-2.33988	-4.03315	-5.87407
H	-3.78795	-3.84668	-4.89154

S=1/2, C₁ point group, full structural model

E(UB3LYP) = -4648.86536711 A.U.

Co	0.00000	0.13635	-0.00003
N	-0.00002	-1.71757	-0.00003
O	-1.90860	0.29069	0.11808
Cl	0.00002	2.55991	0.00002
O	1.90860	0.29067	-0.11812
C	-1.06068	-2.44215	-0.57825
C	1.06063	-2.44216	0.57819
C	-2.81499	-0.78343	0.26388
Li	-2.38681	2.12222	0.25447
Li	2.38684	2.12219	-0.25448
C	2.81498	-0.78346	-0.26391

C	-2.42239	-2.06080	-0.48881
C	-0.76598	-3.60826	-1.33004
C	2.42235	-2.06083	0.48876
C	0.76592	-3.60826	1.33000
C	-4.16046	-0.19546	-0.26922
C	-2.97693	-1.08207	1.78779
O	-2.80939	3.32086	1.76928
O	-3.22383	3.55082	-0.87497
O	2.80941	3.32083	-1.76928
O	3.22391	3.55076	0.87496
C	4.16043	-0.19553	0.26928
C	2.97697	-1.08210	-1.78783
C	-3.40857	-2.88110	-1.06962
C	-1.75279	-4.38554	-1.90816
H	0.27120	-3.88112	-1.45231
C	3.40852	-2.88110	1.06962
C	1.75272	-4.38552	1.90815
H	-0.27127	-3.88111	1.45227
F	-4.36117	1.11661	0.21203
F	-4.15529	-0.07169	-1.65567
F	-5.32269	-0.88483	0.07497
F	-3.90462	-2.09115	2.05420
F	-1.77828	-1.47796	2.36439
F	-3.40249	0.04486	2.51386
C	-2.05584	3.22880	3.01661
C	-2.92156	4.66255	1.21320
C	-3.81918	4.55185	0.00087
C	-3.90885	3.36444	-2.14662
C	2.92164	4.66251	-1.21320
C	2.05584	3.22880	-3.01660
C	3.90895	3.36434	2.14659
C	3.81928	4.55177	-0.00089
F	4.36116	1.11658	-0.21186
F	4.15517	-0.07187	1.65574
F	5.32267	-0.88489	-0.07486
F	3.40273	0.04477	-2.51387
F	3.90450	-2.09133	-2.05422
F	1.77828	-1.47780	-2.36451
C	-3.10900	-4.04383	-1.77546
H	-4.44976	-2.62046	-0.96419
H	-1.47191	-5.26445	-2.47674
C	3.10893	-4.04381	1.77549
H	4.44971	-2.62045	0.96422

H	1.47182	-5.26441	2.47675
H	-1.01127	3.49443	2.84592
H	-2.13173	2.19396	3.33219
H	-2.50206	3.87994	3.77155
H	-3.36547	5.33847	1.95046
H	-1.92952	5.02597	0.93217
H	-4.82450	4.23314	0.29062
H	-3.87834	5.51501	-0.51566
H	-3.36762	2.58446	-2.67133
H	-3.88363	4.28972	-2.72681
H	-4.94205	3.04979	-1.98628
H	1.92962	5.02596	-0.93214
H	3.36556	5.33842	-1.95046
H	2.50206	3.87994	-3.77154
H	1.01128	3.49447	-2.84588
H	2.13169	2.19397	-3.33219
H	3.88377	4.28961	2.72679
H	4.94213	3.04966	1.98623
H	3.36770	2.58438	2.67131
H	4.82458	4.23302	-0.29065
H	3.87849	5.51492	0.51565
C	-4.19602	-4.89803	-2.38704
C	4.19594	-4.89799	2.38711
H	-5.18526	-4.48863	-2.17852
H	-4.17250	-5.91905	-1.99619
H	-4.08952	-4.96628	-3.47352
H	5.18518	-4.48860	2.17861
H	4.17243	-5.91903	1.99629
H	4.08941	-4.96622	3.47360

S=3/2, C₂ point group, simplified model

Co	0.00000	0.00000	0.69814
N	0.00000	0.00000	-1.21291
O	-0.03932	1.95252	0.84624
Cl	0.00000	0.00000	3.27739
O	0.03932	-1.95252	0.84624
C	0.69193	0.99730	-1.92163
C	-0.69193	-0.99730	-1.92163
C	0.00000	2.84699	-0.24653
Li	-0.32541	2.48953	2.66949
Li	0.32541	-2.48953	2.66949
C	0.00000	-2.84699	-0.24653
C	0.76477	2.35536	-1.49344
C	1.41429	0.63826	-3.08857

C	-0.76477	-2.35536	-1.49344
C	-1.41429	-0.63826	-3.08857
C	0.64795	4.13428	0.36151
C	-1.46995	3.18581	-0.65862
O	1.08697	2.76293	3.93804
O	-2.11203	3.00003	3.03589
O	-1.08697	-2.76293	3.93804
O	2.11203	-3.00003	3.03589
C	-0.64795	-4.13428	0.36151
C	1.46995	-3.18581	-0.65862
C	1.49994	3.27320	-2.26789
C	2.14363	1.55858	-3.82246
H	1.39534	-0.39763	-3.39218
C	-1.49994	-3.27320	-2.26789
C	-2.14363	-1.55858	-3.82246
H	-1.39534	0.39763	-3.39218
F	0.12035	4.40459	1.64246
F	2.01448	3.98206	0.55645
F	0.45911	5.31562	-0.35862
F	-1.56199	4.03886	-1.75188
F	-2.19130	2.04395	-0.96464
F	-2.20115	3.82686	0.37932
H	1.37243	1.86980	4.19774
H	1.79954	3.41512	3.96020
H	-2.66930	2.85951	3.81045
H	-2.59078	3.37605	2.28148
H	-1.79954	-3.41512	3.96020
H	-1.37243	-1.86980	4.19774
H	2.59078	-3.37605	2.28148
H	2.66930	-2.85951	3.81045
F	-0.12035	-4.40459	1.64246
F	-2.01448	-3.98206	0.55645
F	-0.45911	-5.31562	-0.35862
F	2.20115	-3.82686	0.37932
F	1.56199	-4.03886	-1.75188
F	2.19130	-2.04395	-0.96464
C	2.18449	2.89573	-3.41665
H	1.53538	4.31206	-1.98505
H	2.68508	1.23540	-4.70223
C	-2.18449	-2.89573	-3.41665
H	-1.53538	-4.31206	-1.98505
H	-2.68508	-1.23540	-4.70223
H	2.74023	3.63201	-3.98009

H -2.74023 -3.63201 -3.98009

12. References

1. Cantalupo, S. A.; Fiedler, S. R.; Shores, M. P.; Rheingold, A. L.; Doerrler, L. H., *Angew. Chem. Int. Ed.* **2012**, *51*, 1000-1005.
2. Rajnak, C.; Titis, J.; Fuhr, O.; Ruben, M.; Boca, R., *Inorg. Chem.* **2014**, *53*, 8200-8202.